J. of the Korean Society for Heat Treatment
Vol.4, No.3, September 1991, pp.21~30

論 文

Microstructure and Fracture Path of Cr-Mn-N Steel upon Aging Treatment

Se-Jong Lee, Jang-Hyun Sung* and K.M. Ralls**
Dept.of Materials sci. and Eng., Kyung Sung Univ.
*Dept. of Metallurgical Engineering, Dong-A Univ.
**The Center of Materials Sci. and Eng., The Univ. of Texas at Austin, U.S.A

ABSTRACT

Microstructural analysis was conducted to observe the effect of aging treatments in a Cr-Mn austenitic stainless steel containing nitrogen, and the amount, size, shape and distribution of precipitates were investigated. It was found that on water quenching from 1000℃ after holding 3 h at that temperature, the steel contained no precipitates observable by optical microscopy. Precipitation of phases begins at places most favorable for the formation of nuclei-in the boundaries of grains and twins. Precipitates were studied in detail by means of scanning electron microscopy (SEM) and transmission electron microscopy (TEM). Chemical compositions of precipitates were examined by the use of scanning transmission electron microscopy (STEM) together with an energy dispersive X-ray (EDX) microanalysis. Also chromium depletion adjacent to grain boundary precipitates was investigated by the use of Auger electron spectroscopy (AES) for a direct examination of the fracture surface chemistry.

I. INTRODUCTION

The investigation of Cr-Mn austenitic stainless steels has resulted in increased searching for a substitute for nickel in alloys, particularly in countries where nickel was in short supply since manganese was more abundant and less expensive. A promising practical substitute, Mn, immediately suggests itself due to its effect on the stability of the austenitic structure, despite the fact that the austenite forming capacity of Mn is weak compared to Ni[1,2]. The lack of this capacity is supplemented by the addition of nitrogen which has intensive austenitic forming capacity. The high nitrogen solubility in steels might be accomplished with a combination of Cr and Mn rather than with either element alone[2].

However, the maximum solubility of nitrogen in equlibrium with austenite is about 0.26 weight percent, so that there is substantial opportunity for the precipitation of nitrides in high-N austenitic stainless steels[3].

The Cr-Mn austenitic stainless steels containing N were widely used in various areas including corrosive environments. Three serious corrosion problems associated with the austenitic grades of stainless steels are stress corrosion cracking, pitting, and sensitization. Many investigators have paid attention to the effect of the heat treatments on the development of intergranular corrosion

cracking in high N steels[4-6]. The austenitic alloys become sensitized during prolonged heating in the general temperature range of 450 to 650℃, and this sensitization causes a marked decrease in the intergranular corrosion resistance which has been explained by the Cr-depletion theory[7,8] This involves precipitation on the grain boundaries and associated depletion of the matrix adjacent to precipitates in Cr, which forms intergranular narrow paths of Cr -depleted austenite of poor corrosion resistance. The inability of the Cr-depleted zone to maintain passivity results in intergranular corrosion in many media in which the stainless steel would ordinarily be resistant.

It has been studied in this paper the microstructural changes and nature of precipitate upon aging treatments, the compositional aspects of the interfaces due to second phase precipitation and the interfaces relationship to the fracture path in a Cr -Mn austenitic stainless steel containing nitrogen.

2. EXPERIMENTAL PROCEDURES

The material used was a Carpenter 18/18 Cr-Mn steel and its chemical composition was as follows : Fe-balance, Cr-18, Mn-18, Ni-0.4, Mo-1.0, C -0.1, N-0.45, Cu-1.0, Si-0.4, P-0.02, and S-0.009 in weight percent. Materials were solutionized at 1000℃ for 3 h followed by water quenching and furnace cooling to room temperature. Aging treatments consisted of heating at both 500℃ and 600℃ for times from 4 h to 1000 h. The specimens were etched using HCl or picric acid diluted with an ethanol for the microstructural observation.

Morphological characteristics of precipitates were observed by electron microscopes. SEM was used to observe the microstructures of the metallographically prepared samples at high magnification, the fracture surfaces and longitudinal sections of Auger specimens after fracture. TEM analysis were made of precipitates isolated in an unchanged state, preserving their original distribution and arrangement, from the specimen aged for 410 h at 600℃ following water quenching. Thin films were prepared by means of a Ni-C double stage extraction replica technique[9,10]. Ni deposition was made electrolytically on samples heavily etched with HCl solution[11,12], and the EDX analysis with SEM was carried out to examine the Ni replica. The second replica film was then applied, by carbon evaporation, on Ni film. Quantitative analysis of precipitates on both the grain and twin boundaries in thin films was conducted by the use STEM.

Auger analysis was made as follows : (1) metallographically prepared specimens ; the SAM technique was applied to examine the bulk composition of the as-solutionized material followed by water quenching, and to investigate the variations in composition across the precipitate on the grain buondary in a 1000 h aged one at 600℃ following water quenching. (2) fracture specimens ; the specimens were initially aged at 600℃ for 256 and 1000 h following water quenching. In-situ point analysis were carried out to investigate the depletion and/or segregation of certain elements (Cr, Mn, Fe, N, C, etc). Quantitative AES analysis was conducted by comparison with standard peaks[13].

3. RESULTS AND DISCUSSION

3.1. MICROSTRUCTURAL OBSERVATIONS

The modifications of microstructure were made by successive precipitation reactions upon aging treatments from supersaturated solutionized condition at elevated temperature. Also the effect of different cooling rates were found to affect initial precipitation reactions, but as the holding time was increased, it was difficult to distinguish such differences.

The as-solutionized condition is shown in Photo 1. The solutionizing treatments with different cooling rates resulted in different microstructures such that the furnace cooled one shows second

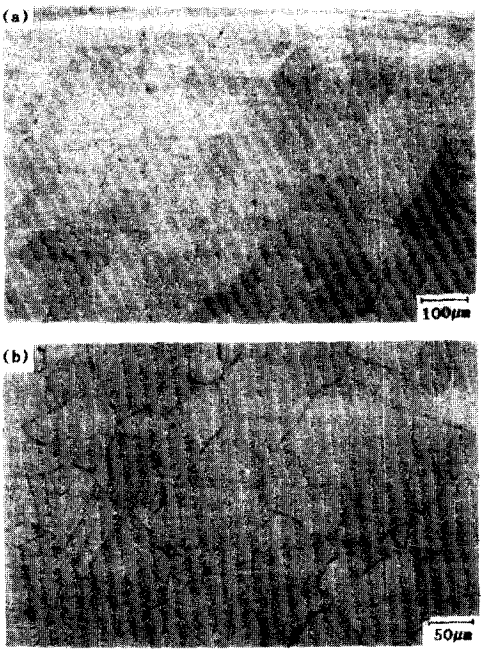

Photo 1. Microstructures of the as-solution treated samples : (a) water quenched, (b) furnace cooled.

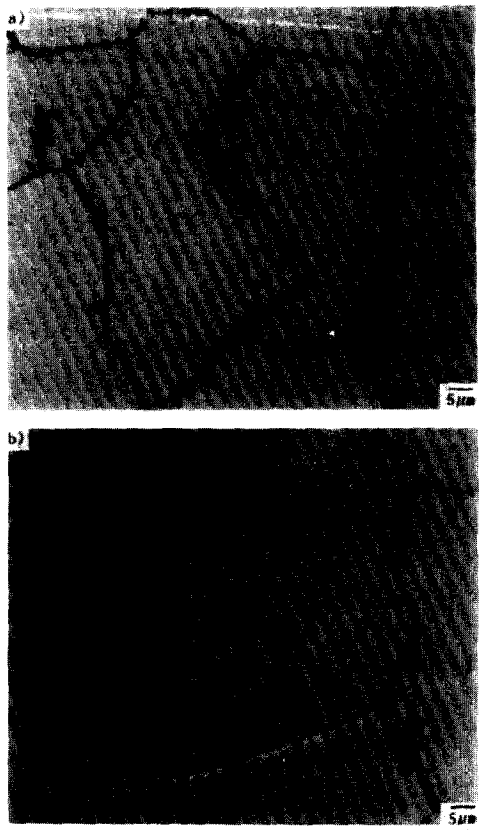

Photo 2. Microstructures of a 1000h aged sample at 600℃ following water quenching.
Etchant : (a) HCl in ethanol, (b) picric acid in ethanol.

phase particles on the grain boundaries, but the water quenched do not contain any precipitates throughout the microstructure. Also it was observed that some degree of serrated grain boundaries is found in the former.

3.1.1. Specimens aged at 600℃

Precipitation was first found in specimens after 4 h aging, and observed to initiate on the grain boundaries, As the holding time was increased, the amount of precipitates was found to be increased and the precipitation on the twin boundaries started. After 16 h aging, small precipitates ard found on the incoherent twin boundaries, but the coherent twin boundaries remain free of precipitates. After longer exposure at this temperature, nodular patches were found along the grain boundaries and the precipitate develops along the coherent twin boundaries. With increasing holding time both grain and twin boundary precipitates are greatly increased in amount and size, and they grow from grain boundaries into the grains. Another precipitation inside grains was found to initiate after a prolonged holding time at this temperature. Photo 2 and 3 show the microstructures of both water quenched and furnace cooled specimen after 1000 h aging treatment at 600℃, respectively. Also they reveal the difference in microstructure resulting from two different etchants. During the observation of microstructural changes upon aging, it was found that the etchant mixed with HCl reveals very well the grain and twin boundaries as well as the precipitates on those sites and the general precipitates within grains. In contrast, the etchant containing picric acid reveals clearly the discontinu-

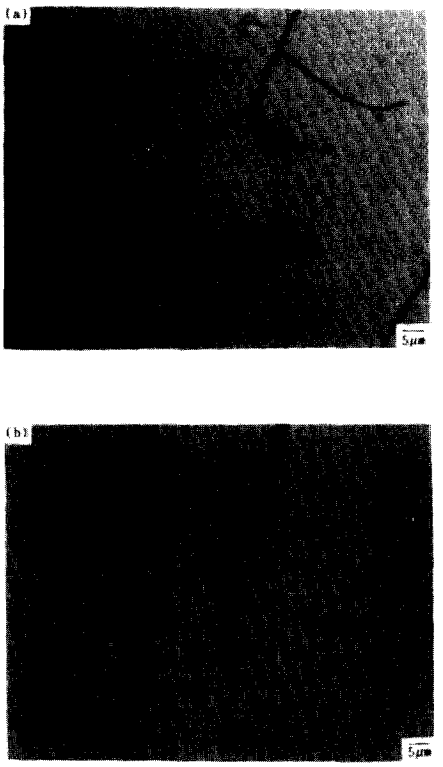

Photo 3. Microstructures of a 1000h aged sample at 600℃ following furnace cooling.
Etchant : (a) HCl in ethanol, (b) picric acid in ethanol.

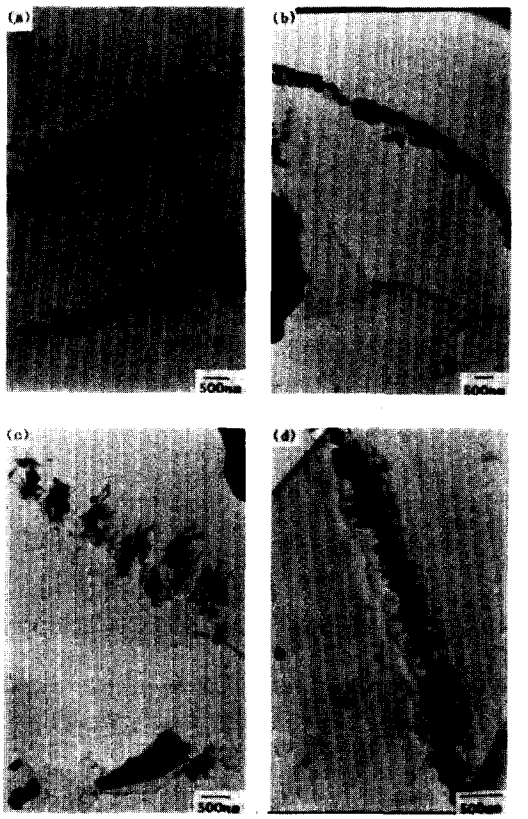

Photo 5. Transmission eletron micrographs of a 410h aged sample at 600℃ following water quenching :
(a)-(c) grain boundary precipitates, (d) twin boundary precipitates.

ous precipitates along the grain boundaries and allows one to resolve the lamellar characteristics as shown in Photo 4(a), and 4(b) which shows some degree of spheroidization in the lamellar areas. The

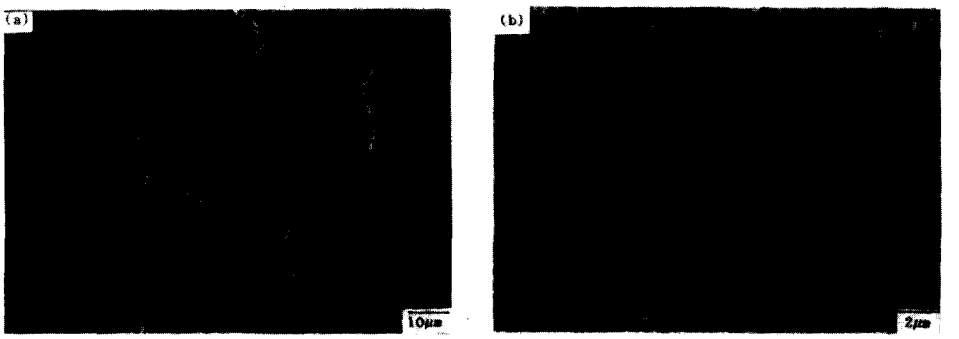

Photo 4. Scanning eletron micrographs of a 1000h aged sample at 600℃ following water quenching (Etchant : picric acid in ethanol).

etchant with HCl outlined such discontinuous lamellar precipitate and only upon very severe etching showed the lamellae, with resulting in some damage to the microstructures.

In an attempt to investigate the morphological aspects of precipitates, a serises of transmission electron micrographs were taken, and these are presented in Photo 5. The shapes of grain boundary precipitates vary from blocky to plates to the form of lamellar precipitates. This transition in precipitate shape was well discussed by H.I.Aaronson and co-workers[14]. Photo.5(a) to 5(c) shows such precipitates along grain boundaries. The precipitation on twin boundaries extends to both sides of a twin parallel to coherent boundaries as elongated needles, as shown in Photo 5(d). Also the widening of twin boundaries occurs by a continuous precipitation, no nodular or lamellar precipitation is observed at these locations. The orientation relationship between the general precipitation and the matrix was not investigated, but the fine, dot-like precipitates in the matrix are expected to form well-defined Widmanstatten arrays on further aging[15].

3.1.2. Specimens aged at 500℃

The precipitation reaction at this relatively low temperature was found to be very much sluggish compared to that at 600℃. The microstructures upon aging treatments are similar to those of specimens aged at 600℃ for much shorter periods of time, and it was observed that the amount of precipitates was so small even after 1000 h aging. However, it is clear in this condition that different cooling histories affect the resulting structures. Specimens that were furnace cooled originally showed precipitates along the twin boundaries, where they were much more uniform throughout the boundaries without marked

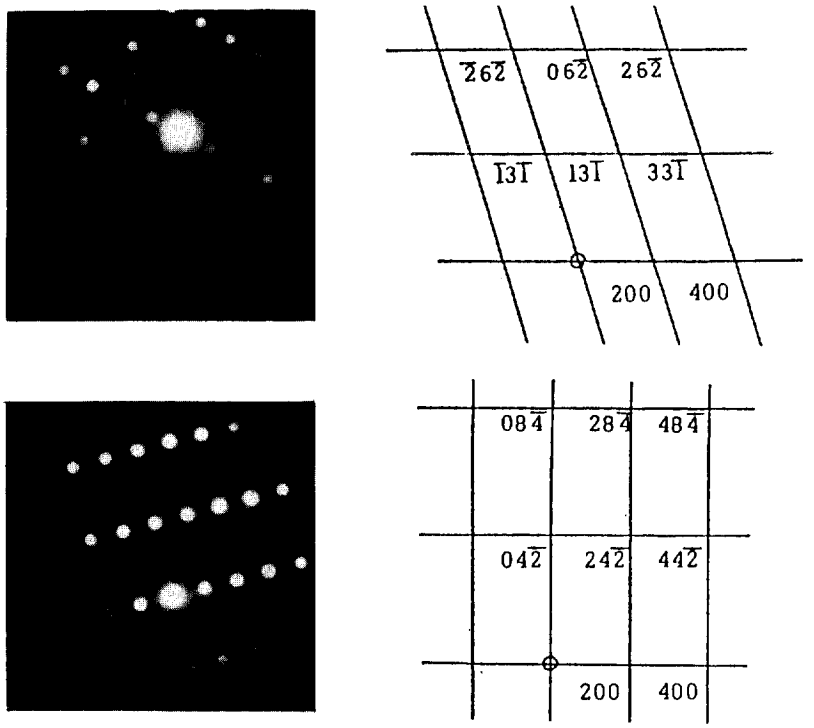

Photo.6. Selected area diffraction patterns from grain boundary precipitates in a 410h aged sample at 600℃ following water quenching.

concentration at the incoherent twin boundaries compared to those at 600℃.

3.2. IDENTIFICATION OF PRECIPITATED PHASES

Selected area diffraction patterns were obtained on the grain boundary precipitates and indexed as given in Photo 6. Analysis by indexing indicates that the precipitate has the fcc $Cr_{23}C_6$ structure. Chemical analysis by STEM with EDX microanalysis indicates that the precipitates both on the grain and twin boundaries contain Cr, Fe, Mo and a very small amount of Si. The EDX spectra are presented with relevant electron micrographs in Fig. 1. The Cu peaks are believed to be come from the Cu grid. The chemical compositions were obtained based upon those spectra and are given in Table 1 with respect to Cr, Fe and Mo. (The relative amount of Si was found to be about 0.05 weight percent and this has not been included.) The concentrations of these elements varies slightly from one site to another, but seems to be almost the same at different locations on either grain bound-

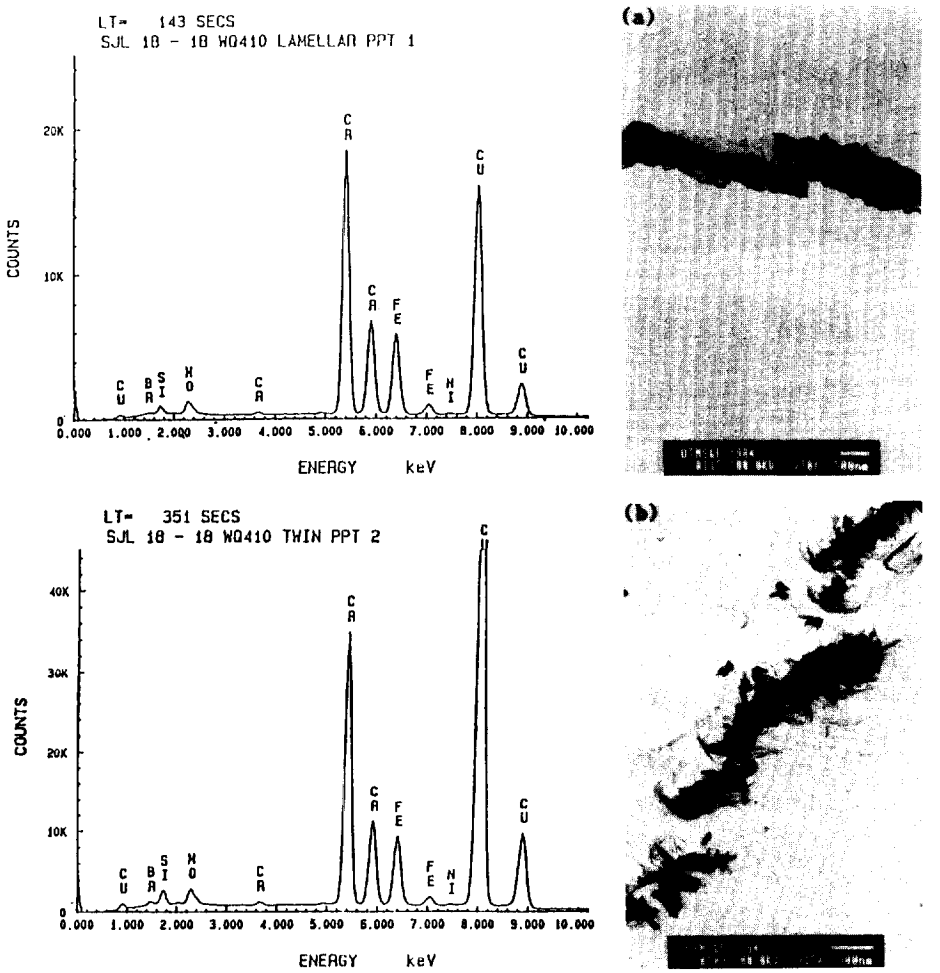

Fig. 1. EDX spectra with relevant STEM photographs of a 410h aged sample at 600℃ following water quenching : (a) grain boundary lamellar precipitate, (b) twin boundary continuous precipitate.

Table 1. Chemcal Compostition of Precipitates of a 410hr. Aged Specimen at 600℃ Following Water Quenching by Means of STEM Microanalysis.

Position/wt%	FE	CR	MO
grain boundary	22.92	69.99	7.07
twin boundary	20.31	70.84	8.83
g.b. lamellar	22.66	70.10	7.23

aries or twin boundaries. The markedly dominant element in those precipitates was found to be Cr, but a considerable amount of Fe and Mo was also found. It was expected that these precipitates might contain Mn, but the analysis did not detect any clear peak of Mn. It is interesting to note that the metal atom compositions of the precipitates are consistent with data for the $M_{23}C_6$ phase in type 316 Cr-Ni austenitic stainless steels investigated by J. K. Lai et al[16]. According to their findings by means of STEM X-ray microanalysis, the grain boundary $M_{23}C_6$ phase contained 18.3% of Fe, 61.0% of Cr, 7.7% of Mo, 11% of Ni and 1.4% of Si in weight percent. The precipitate composition in the current study differs from that reported by J.K.Lai et al, mainly because of the presence of Mn rather than Ni in the alloy being studied. So if the Ni present in the carbide of the type 316 stainless steel were replaced by Cr because of relatively very small content of Ni in this material, it could be said that those carbide precipitates on both materials seemed to have similar compositions. It is believed that with an increasing duration time the enrichment of the precipitate in Cr, associated with a steady replacement of Fe atoms in the carbide lattice by atoms of Cr takes place and results in an increase in the lattice constant of the precipitate since Cr possesses a somewhat larger atomic radius[17,18].

The STEM analysis did not include the light elements such as carbon and nitrogen. Auger line profiles were obtained, especially to find out the possibility of the presence of N in the precipitate, across a huge lamellar precipitate along the grain

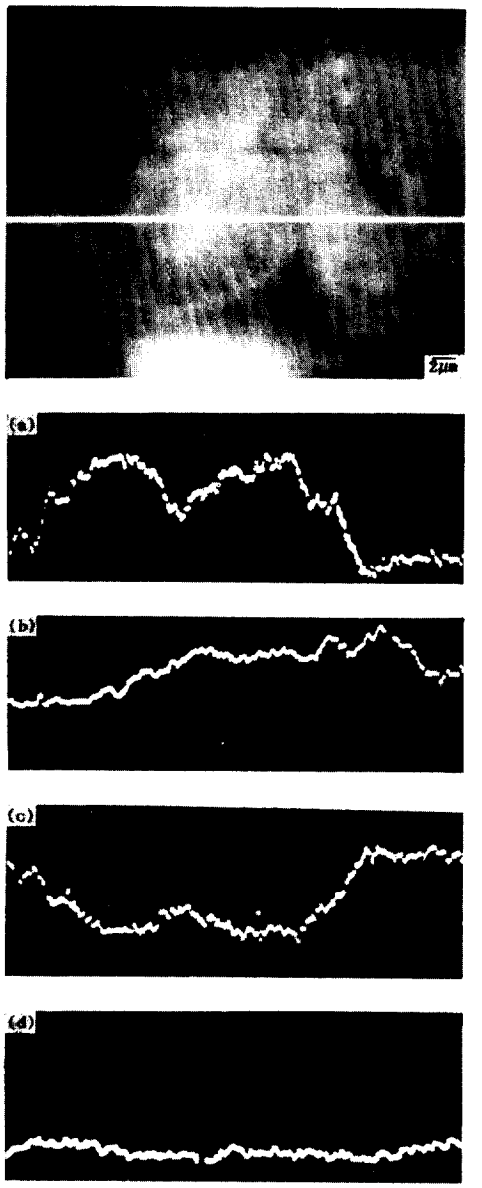

Photo 7. Auger nline profiles with a relevant SAM photograph of a 1000h aged sample at 600℃ following water quenching : (a)Fe, (b)Cr, (c)C, (d)N.

boundary and presented in Photo 7. This experiment shows that the relative peak heights of C and Cr increas noticeably and the Fe peak height drops sharply inside the area of lamellar precipitate. It looks to be no change in N peak. Because of the large beam size, about 1.0 mm, compared to the

thickness of each lamella, about 0.3 mm, it is meaningless to discuss these results quantitatively.

3.3. ANALYSIS ON FRACTURE PATHS

With an aid of SEM, the fracture surface was observed clearly and found to be a mixed trans-granular-intergranular mode with a higher fraction of intergranular fracture. The SEM fractographs are shown in Photo 8. The relative amount of such intergranularlly fractured region is much higher in a 1000 h aged sample than that in a 256 h aged one, and also the former shows many facets which have dimples and roughness compared to thd latter that has relatively smooth intergranular facets. At this point, it is important to recall that the 1000 h aged specimen contains a much greater amount of grain boundary lamellar precipitates. The fracture properties and effect of lamellar precipitates in Cr-Mn austenitic steels were investigated by others[19,20]. They found that ductility decreases considerably with an increase of grain boundary reaction nodules owing to the brittle fracture of lamellae. In the present study, microstructure of longitudinal sections of fractured specimens showed intergranular, secondary cracking beyond the fracture surface.

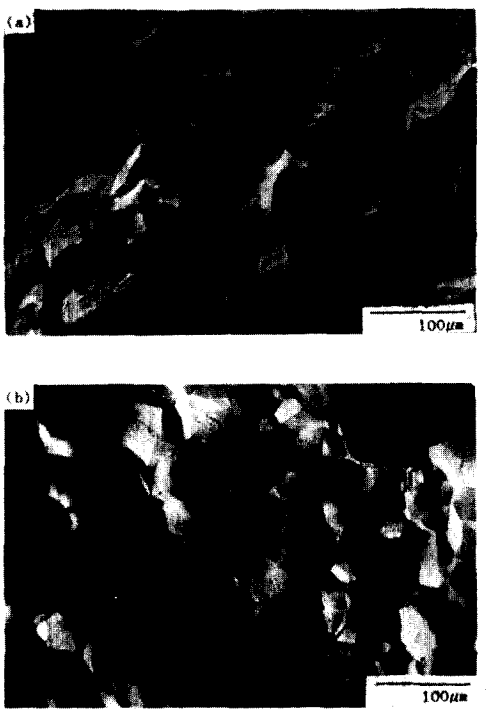

Photo 8. Scanning electron fractographs of aged sample at 600℃ following water quenching : (a) 256h, (b) 1000h.

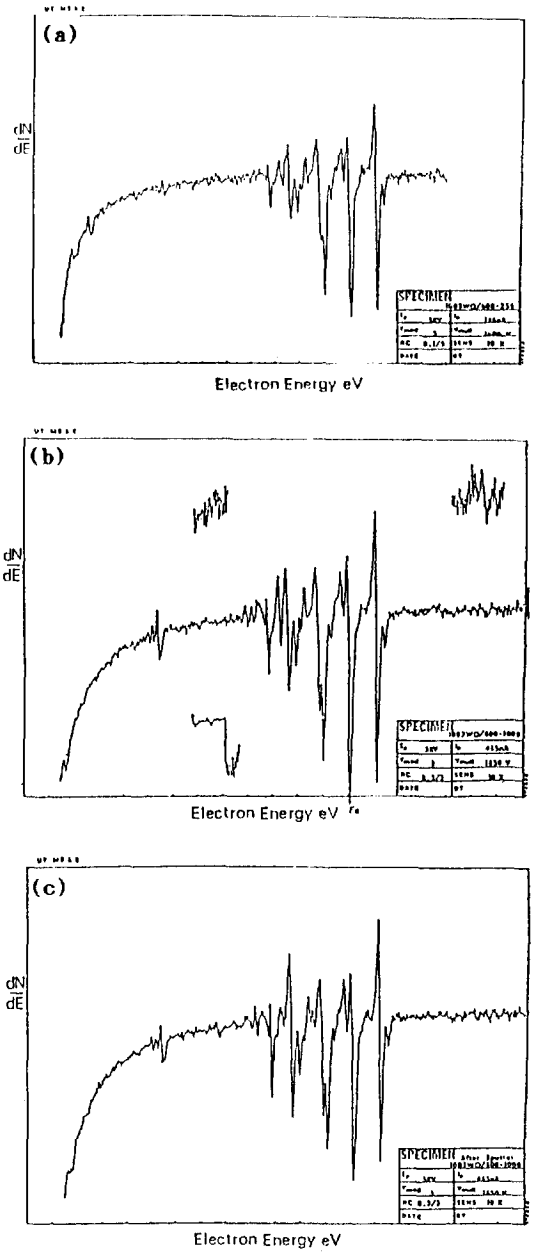

Fig. 2. Auger spectra of fracture surface in aged sample at 600℃ following water quenching : (a) 256h before sputtering, (b) 1000h before sputtering, (c) 1000h after sputtering.

With the observable concentration limits of AES being approximately 0.1 atomic percent, certain minor elements such as P and S should not be seen on an Auger spectrum unless something has occurred to increase the concentration in the region the analysis was conducted[21]. The Auger spectra obtained are given in Fig.2, and the calculated compositions from those spectra are presented in Table 2. The spectra taken from the aged specimens show a P peak. This might indicate segregation of P due to heat treatment. The quantitative data show an increase in P on the fracture surface for the 256 h aging but back to the bulk concentration for the 1000 h aging. This might indicate the fracture of that specimen was influenced by the segregation of P, but it is thought that after longer aging time the P might diffuse back away from the grain boundary into the matrix, or be forced out of grain boundaries because of grain boundary precipitates. Also there appears to be a depletion of Cr on the fracture surface of aged specimens with respect to the as-solutionized specimen. The degree of Cr-depletion in the 1000 h aged specimen appears to be slightly larger than that of 256 h aged one, but it is hard to say that there is a real difference in an amount of Cr because of the large standard deviation. In the same context, there are an enrichment of Mn and depletions of Fe and N on the aged specimens fracture surface. The Fe depletion and Mn enrichment could result from second phase precipitation[4], but the apparent enrichment may be a consequence of the overlap of the Mn 589 eV and the Fe 598 eV peak. After argon sputtering the fracture surface of the 1000 h aged sample, it's apparent from Table 2 and Fig.2(b)-(c) that the depletion of Cr and N are very localized at the fracture surface. The Cr and N depletion may be attributed to the formation of chromium carbide which contains nitrogen. The variations in concentrations of C and Mn cannot be explained. The surface area composition may not be uniform and observation from one selected point during sputtering may not be consistent with surface variations. The fractures are not smooth and that might affect the AES spectrum. The investigation of depletion and/or enrichment of elements upon heat treatment is well accomplished with thin films by means of STEM microanalysis[22].

Table 2. Summary of the Auger Data of the Specimens Aged at 600℃. (wt.%)

	Comp.	As quenched	Fractured (256 hr)	Fractured (1000 hr)	Fractured and Sputtered
Fe	60.62	57.2±1.6	50.0±2.3	54.1±1.9	47.70
Cr	18	18.4±0.7	14.8±1.2	11.4±4.1	20.50
Mn	18	17.1±1.1	23.9±0.5	24.2±0.4	23.20
C	0.10	2.33±0.6	2.40±0.6	2.10±0.9	2.40
N	0.45	0.84±0.15	-	-	0.79
Ni	0.4	-	-	1.20±0.5	1.00
Mo	1.0	3.08±1.25	2.00±1.6	-	1.70
Cu	1.0	0.61±1.08	-	4.20±2.1	2.50
Si	0.4	0.12±0.23	-	-	0.30
P	0.02	0.20±0.25	1.41±0.7	0.35±0.37	-
S	0.009	0.11±0.11	-	-	-

The investigations on fracture surfaces using Auger spectroscopy can be connected to the results obtained by means of electron microscopy such that the precipitated phase along the grain boundaries must be the carbide containing mainly Cr, C and a relatively small amount of Fe and, possibly, N $M_{23}C_6$ carbide containing nitrogen was reported in Cr-Mn-N steels by E.J.Dulis et al[15].

4. CONCLUSIONS

1) The aging treatments at 500℃ and 600℃ cause successive precipitations on the grain boundaries, twin boundaries and finally within grains. The discontinuous grain boundary precipitation was resolved as the pearlitic lamellar precipitate.

2) The precipitation reaction upon aging at both 500℃ and 600℃ is found to continue even after 1000 h holding time. On aging at 600℃, the reaction is

much more complete than at 500℃.

3) The precipitate is thought to be the same type, both on the grain and twin boundaries, and found to contain the relative amount of Cr-70.3%, Fe-22.0% and Mo-7.7% in average weight percent omitting the carbon.

4) The only precipitate positively identified is the $M_{23}C_6$-type carbide.

5) The long term aging treatments couse the intergranular fracture along regions depleted in Cr and N. In some conditions, P is segregated to grain boundaries upon aging.

5. REFERENCES

1. O.A.Bannykh, Met. Term. Ob. Metal. No.7, pp.7-10 (1980).
2. J.J.Heger, ASTM STP 369, pp.54-61 (1963).
3. C.Hsiao and E.J.Dulis, Trans. ASM vol.52, pp.855-877 (1959).
4. B.R.Nijhawan, P.K.Gupte, S.S.Bhatnagar, B. K.Guha, and S.S.Dhanjal, JISI, pp.292-303 (1967).
5. G.F.Torkhov, V.A.Slyshankova, E.A.Ul' yanin, and A.V.Sherevera, Met. Term. Ob. Metal. No.11, pp.8-11 (1978).
6. T.V.Rashev, L.P.Dzhambazava, R.St.Kovacheva, and Ch.A.Andreev, Met. Term. Ob. Metal.No.5, pp.13-15 (1981).
7. M.G.Fontana and N.D.Greens, "Corrosion Engineering," McGraw-Hill Book Co., pp.58-60 (1978).
8. E.M.Mahla and N.A.Nielsen, Trans. ASM vol. 43, pp.290-322 (1951).
9. M.V.Heimendahl, Electron Microscopy of Materials, Academic Press, London, England, 1980, pp.74-89.
10. G.Henry and J.Plateau, Met. Scl. Rev. No.2, pp.129-135 (1964).
11. W.Blum, "Principles of Electroplating and Electroforming," McGraw-Hill Book Co., pp.362-381 (1949).
12. W.L.Pinner, G.Soderberg, and E.M.Baker, "Modern Electroplating," The Electrochemical Society, pp.235-274 (1942).
13. H.L.Marcus and D.Finello, "Electron and Positron Spectroscopies in Materials Sciences and Engineering," Academic Press, pp.121-181 (1979).
14. H.I.Aaronson, H.B.Aaron, and K.R.Kinsman, Metallography vol.4, pp.1-42 (1971).
15. C.Hsiao and E,J.Dulis, Trans. ASM, vol.49, pp.655-685 (1956).
16. J.K,Lai, D.J,Chastell, and P.E.J.Flewitt, "Solid-State Phase Transformations," AIME, pp.781-785 (1981).
17. J.K.Mukherjee and B.R.Nijhawan, JISI, pp.62-69 (1967).
18. V.M.Farber, A.M.Oparina, B.M. Bronfin, Yu.P.Bulanov, A.A.Popov, G.V.Kuznetsova, and A.V.Shustov, FMM vol.45, pp.114-117 (1978).
19. M.Tanaka and T.Sakaki, J. Mat. Sci. vol.13, pp.1658-1670 (1978).
20. J.Albrecht, Script. Met. vol.17, pp.371-374 (1983).
21. A.Joshi, "Interfacial Segregation," ASM, pp.39-109 (1977).
22. P.Doig and P.E.J.Flewitt, J. Microsc. Spectro. Electron. vol.8, pp.193-210 (1983).